Biochimica et Biophysica Acta 1833 (2013) 629–642

Contents lists available at SciVerse ScienceDirect

Biochimica et Biophysica Acta

journal homepage: www.elsevier.com/locate/bbamcr

The COOH-terminus of TM4SF5 in hepatoma cell lines regulates c-Src to form invasive protrusions *via* EGFR Tyr845 phosphorylation

Oisun Jung [a,1], Yoon-Ju Choi [b,1], Tae Kyoung Kwak [b], Minkyung Kang [c], Mi-Sook Lee [b], Jihye Ryu [b], Hye-Jin Kim [b], Jung Weon Lee [a,b,*]

[a] *Interdisciplinary Program in Genetic Engineering, Seoul National University, Seoul 151-742, Republic of Korea*
[b] *Department of Pharmacy, Research Institute of Pharmaceutical Sciences, Medicinal Bioconvergence Research Center, College of Pharmacy, Seoul National University, Seoul 151-742, Republic of Korea*
[c] *Department of Biomedical Sciences, College of Medicine, Seoul National University, Seoul 110-799, Republic of Korea*

ARTICLE INFO

Article history:
Received 9 July 2012
Received in revised form 26 November 2012
Accepted 29 November 2012
Available online 6 December 2012

Keywords:
EGFR
Hepatocarcinoma
Invasion
Src family kinase
TM4SF5

ABSTRACT

Transmembrane 4 L six family member 5 (TM4SF5) enhances cell migration and invasion, although how TM4SF5 mechanistically mediates these effects remains unknown. In the study, during efforts to understand TM4SF5-mediated signal transduction, TM4SF5 was shown to bind c-Src and thus hepatoma cell lines expressing TM4SF5 were analyzed for the significance of the interaction in cell invasion. The C-terminus of TM4SF5 bound both inactive c-Src that might be sequestered to certain cellular areas and active c-Src that might form invasive protrusions. Wildtype (WT) TM4SF5 expression enhanced migration and invasive protrusion formation in a c-Src-dependent manner, compared with TM4SF5-null control hepatoma cell lines. However, tailless TM4SF5$_{\Delta C}$ cells were more efficient than WT TM4SF5 cells, suggesting a negative regulatory role by the C-terminus. TM4SF5 WT- or TM4SF5$_{\Delta C}$-mediated formation of invasive protrusions was dependent or independent on serum or epidermal growth factor treatment, respectively, although they both were dependent on c-Src. The c-Src activity of TM4SF5 WT- or TM4SF5$_{\Delta C}$-expressing cells correlated with enhanced Tyr845 phosphorylation of epidermal growth factor receptor. Y845F EGFR mutation abolished the TM4SF5-mediated invasive protrusions, but not c-Src phosphorylation. Our findings demonstrate that TM4SF5 modulates c-Src activity during TM4SF5-mediated invasion through a TM4SF5/c-Src/EGFR signaling pathway, differentially along the leading protrusive edges of an invasive cancer cell.

1. Introduction

Cancer metastasis is dynamically regulated by coordinated signaling pathways that respond to the extracellular matrix (ECM) or soluble factors [1]. Cell migration involves new focal adhesions or contacts in the leading edges, adhesion-dependent regulation of RhoA GTPase activity, intracellular contractility, actin reorganization, and disassembly of focal adhesions in rear edges [1]. Invasion involves degradation of the ECM *via* formation of invasive morphological features depending on cell adhesion signaling activity [2].

Cell adhesion causes tyrosine phosphorylations and activations of diverse molecules at focal adhesions (FAs, [3]). Among these FA molecules, focal adhesion kinase (FAK) is autophosphorylated at Tyr397 when cells adhere. Phosphorylated Tyr397 recruits Src-homology 2 (SH_2)-domain containing molecules like c-Src, which phosphorylates other Tyr residues in FAK [4]. The FAK–c-Src complex is thus involved importantly in modulating diverse signaling pathways after cells adhere [5]. c-Src is a well-known tyrosine kinase involved in cell adhesion and/or growth factor receptor (GFR)-mediated signal transduction. c-Src Tyr416 phosphorylation by the FAK-Src complex upon cell adhesion results in its activation, whereas Tyr527 phosphorylation by Src tyrosine kinase (Csk) leads to inactivation [6]. During activation of epidermal growth factor receptor (EGFR), tyrosines 992, 1068, 1086, 1148, and 1173 are autophosphorylated after epidermal growth factor (EGF) interaction [7]. Cell adhesion-activated c-Src can also phosphorylate EGFR in a different pattern for tyrosines 845, 891, 920, and 1101 even without EGF binding [8].

Invasive morphological features including invadopodia and invasive protrusions sense the ECM around the leading edges of a cell and involve adhesion-dependent signaling activities [9]. Such invasive features involve dynamic actin remodeling: c-Src-mediated cortactin phosphorylation causes activation of Arp2/3, consequently leading to actin branching and polymerization at lamellipodia and invasive protrusions [10].

Abbreviations: ICL, intracellular loop; SYF, c-Src-, Fyn-, and Yes-negative mouse embryonic fibroblasts; SYF++, c-Src-reconstituted SYF cells; SFKs, c-Src family kinases; TERM, tetraspanin-enriched microdomain; TM4SF5, Transmembrane 4 L6 family member 5; TM4SF5$_{\Delta C}$, COOH-terminus-deleted TM4SF5

* Corresponding author at: College of Pharmacy, Seoul National University, Seoul 151-742, Korea. Tel.: +82 2 880 2495; fax: +82 2 872 1795.
E-mail address: jwl@snu.ac.kr (J.W. Lee).

[1] These authors contributed equally to this work.

0167-4889/$ – see front matter © 2012 Elsevier B.V. All rights reserved.
http://dx.doi.org/10.1016/j.bbamcr.2012.11.026

Tetraspanins or transmembrane 4 super-family members (TM4SFs) are suggested to locate at the tetraspanin-enriched microdomains (TERMs) of the cell membrane [11] and collaborate with integrins for cell adhesion and migration [12]. Transmembrane 4 L six family member 5 (TM4SF5) is a membrane glycoprotein with four transmembrane domains, and its intracellular loop and N- and C-terminal tails are located in the cytosol [13]. TM4SF5 is highly expressed in diverse clinical cancer tissues, and its overexpression causes aberrant proliferation, angiogenesis, migration, and invasion [14]. However, it is unknown how TM4SF5 mechanistically mediates its tumorigenic effects and which intracellular signaling pathways are emanated from TM4SF5. During studies on TM4SF5-mediated signaling, we found c-Src as a physical binder of the C-terminal tail of TM4SF5, which became the pivotal data of this study.

We hypothesized that TM4SF5 might regulate c-Src for cell invasion and thus examined how TM4SF5 could regulate c-Src activity and invasive features. We found that the C-terminus of TM4SF5 interacted with both active and inactive c-Src. Wildtype (WT) or C-terminus-deleted TM4SF5$_{\Delta C}$ resulted in activation of c-Src and enhanced formation of invasive protrusions. Furthermore, these TM4SF5-mediated effects depended on Tyr845 phosphorylation of EGFR. TM4SF5, c-Src suppression, or Y845F EGFR mutation abolished the invasive protrusions formation, indicating a regulatory signal link from TM4SF5/c-Src complex to EGFR during cell invasion.

2. Materials and methods

2.1. Cell culture

Control (SNU449, SNU761 parental, and SNU761-mock), TM4SF5 WT (SNU449-TM4SF5 and SNU761-TM4SF5 WT), or mutant (SNU761-TM4SF5 ΔICL13, ΔICL19, or TM4SF5$_{\Delta C}$)-expressing human hepatocellular carcinoma cells were described previously [15] or prepared by G418 (A.G. Scientifics, Waltham, MA, USA) selection following transfection of FLAG-mock, -TM4SF5 WT, -TM4SF5 ΔICL13, TM4SF5 ΔICL19, or TM4SF5-$_{\Delta C}$ plasmids into TM4SF5-null SNU449 or SNU761 hepatoma cell lines. Stable cells were maintained in RPMI-1640 (WelGene, Daegu, Korea) containing 10% FBS, G418 (250 μg/ml) and antibiotics (Invitrogen, Carlsbad, CA, USA). Endogenously TM4SF5-null SNU398, SNU449, and SNU761 or TM4SF5-expressing SNU368, HepG2, and Huh7 hepatoma cell lines were maintained in DMEM-H or RPMI-1640 (WelGene) containing 10% FBS and antibiotics (Invitrogen). SYF (c-Src, Yes, and Fyn-negative) and SYF++ (SYF reconstituted with c-Src) cells that endogenously express TM4SF5 were kindly gifted by Dr. Lee Graves (Dept. of Pharmacology, Univ. of North Carolina at Chapel Hill, NC, USA).

2.2. Peptides, cDNAs, siRNA, and shRNA

Peptides ^{1}MCTGKCARCV^{10} (N-terminally cytosolic), ^{69}RAGGKGC CGAGCCGNRCRMLRSV^{91} (intracellular loop, ICL), or ^{187}GDCRKKQD TPH^{197} (C-terminally cytosolic) were commercially synthesized to contain N-terminally-linked biotin without modifications and then purified (90%, Peptron Inc.). The TM4SF5 cDNA sequence (NM-003963, 197 aa) was conjugated to the FLAG tag, and deletion mutations in the intracellular loop or C-terminus were generated to produce ^{69}RA–^{90}SV (ΔICL19 with a deletion of ^{71}GGKGCCGAGCCGNRCRMLR^{89}), ^{69}RAGGK–^{87}MLRSV (ΔICL13 with a deletion of ^{74}GCCGAGCCGNRCR^{86}), or C-terminal tail (^{187}GDCRKKQDTPH^{197})-deleted (ΔC) TM4SF5. GST-TM4SF5, myc-$(His)_6$-TM4SF5, FLAG-TM4SF5, FLAG-TM4SF5 ΔICL13, FLAG-TM4SF5 ΔICL19, or FLAG-TM4SF5$_{\Delta C}$, and Y845F EGFR constructs were engineered and confirmed by direct sequence analyses. GST-c-Src WT, -SH_3, -SH_2, or -SH_2SH_3 constructs were also previously described [16], and pKH_3-$(HA)_3$-c-Src WT, K295R, Y416F, or Y527F mutants were previously explained [17]. siRNA against c-Src was previously explained [18]. shRNAs against TM4SF5 or control sequence are previously explained, and control shRNA was designed for a scrambled sequence [15].

2.3. Extract preparation and Western blots

Subconfluent cells in media containing 10% FBS or cells transiently transfected with the indicated plasmids for 48 h were harvested for whole cell lysates. Cells were transiently transfected with shRNA against control scrambled sequence or TM4SF5 (shTM4SF5) or pFLAG (Mock), pEGFP (GFP), Myc-$(His)_6$-TM4SF5 (MH-TM4SF5), FLAG-TM4SF5 WT, intracellular loop deleted (ΔICL13 or ΔICL19), C-terminal deleted (ΔC) TM4SF5 mutant, pKH_6-$(HA)_3$-c-Src WT, inactive c-Src Y416F, constitutively active c-Src Y527F, kinase-dead c-Src K295R mutant plasmids for 48 h, prior to harvests or replating as previously explained [19]. The cells were harvested using a lysis buffer containing 1% Brij58, 150 mM NaCl, 20 mM HEPES, pH 7.4, 2 mM $MgCl_2$, 2 mM $CaCl_2$, and protease inhibitors. Primary antibodies used include anti-pY^{397}FAK (Abcam, Cambridge, UK), pY^{577}FAK (Invitorgen), pY^{416}Src, pY^{527}Src, pY^{845}EGFR, pY^{992}EGFR (Cell Signaling Technol. Danvers, MA, USA), pY^{486}Cortactin (Millipore, Bellerica, MA, USA), α-tubulin, FLAG, talin, (Sigma, St Louis, MO, USA), pY^{118}paxillin, c-Src, pY^{1173}EGFR, $(His)_6$, HA, pY^{925}FAK (Santa Cruz Biotech., Santa Cruz, CA, USA), GST, paxillin, FAK (BD Transduct. Lab., Bedford, MA, USA), or TM4SF5 [homemade [15]]. The density ratio was evaluated by image J determination.

2.4. Cell surface protein analysis

Localization of TM4SF5 WT and FLAG-TM4SF5$_{\Delta C}$ mutant on plasma membranes was analyzed using Pierce® Cell Surface Isolation Kit (Pierce, Rockford, IL), as previously explained [20]. Subconfluent cells biotinylated for 30 min at 4°C with ensuring even coverage of the cells with the labeling solution of the kit were harvested for preparation of biotinylated surface protein samples, prior to immunoblotting against the indicated molecules. Coimmunoprecipitation between FLAG-TM4SF5 WT or -TM4SF5$_{\Delta C}$ mutant and other proteins using membrane fractions were also performed. The membrane fraction was prepared by ProteoExtract® Subcellular Proteome Extraction Calbiochem® kit following the manufacturer's protocols. Briefly, subconfluent cells in 10 mm tissue culture dishes were twice washed with the Wash buffer of the kit with a gentle rocking for 5 min at 4°C. The cells were covered with Extraction buffer I with protease inhibitor cocktail for 10 min at 4°C with gentle rocking. After removal of the supernatant, the remaining cellular materials were incubated with Extraction buffer II with protease inhibitor cocktail for 30 min at 4°C with gentle rocking. The supernatant was transferred to a new tube for protein determination and immunoblotting or immunoprecipitation using anti-FLAG antibody (Sigma).

2.3. In vitro pull down

In vitro pull down using biotin-conjugated peptides of the cytosolic TM4SF5 regions or recombinant GST-fused c-Src proteins and cell extracts was performed using streptavidin agarose beads (Millipore), as previously described [19]. The biotin–peptides (1 μM) was incubated with SNU449 parental cell extracts (500 μg proteins) or recombinant GST alone, GST–c-Src WT, or -c-Src fragments overnight, prior to precipitation with streptavidin-agarose and standard Western blots.

2.4. Coimmunoprecipitation

Whole cell extracts were prepared using the lysis buffer from TM4SF5-null SNU449 or SNU761 parental hepatoma cells expressing Myc-$(His)_6$-mock, Myc-$(His)_6$-TM4SF5, FLAG-mock, FLAG-TM4SF5, pKH_3-$(HA)_3$-c-Src WT, pKH_3-$(HA)_3$-c-Src Y416F, pKH_3-$(HA)_3$-c-Src

Y527F, or pKH_3-$(HA)_3$-c-Src K295R mutant in the indicated combination for 48 h. The whole cell lysates or membrane fractions as explained above were immunoprecipitated with anti-FLAG antibody-precoated agarose beads (Sigma), c-Src, or -EGFR antibody overnight, prior to immunoblotting for the indicated molecules. Alternatively, cell extracts were incubated with anti-$(His)_6$ antibody overnight prior to protein A/G bead precipitation at 4°C for 2 h. Washed immunoprecipitated proteins were processed to standard Western blots.

2.5. Indirect immunofluorescence

Cells were transiently transfected with FLAG-TM4SF5 WT or $TM4SF5_{\Delta C}$ mutant for 48 h, prior to a double-staining using antibody against phospho-Y^{527}c-Src and FLAG, or phospho-Y^{845}EGFR and FLAG.

2.6. Transwell migration or invasion assay

SNU449 or SNU761 cells stably or SYF or SYF++ mouse embryonic fibroblasts cells transiently transfected with FLAG (mock), FLAG-TM4SF5 WT or -$TM4SF5_{\Delta C}$ mutant were analyzed for migration or invasion, as explained previously [21]. The migration assay was performed for migration toward 10% FBS separately for 12, 16, or 24 h. The invasion through matrigel was done for 36 h using a transwell chamber system, whose bottom chamber side contained culture media with 10% FBS in the absence or presence of 100 ng/ml EGF (PeproTech, Rocky Hill, NJ, USA).

2.7. Invasive protrusion analysis

Cells without or with transient transfection of FLAG (mock), FLAG-TM4SF5 or mCherry-TM4SF5 WT, or FLAG-$TM4SF5_{\Delta C}$ or mCherry-$TM4SF5_{\Delta C}$ mutant were analyzed for invasive protrusions by culturing cells on Oregon Green® 488-conjugated gelatin (Invitrogen), prior to seeing the black spots following degradation of gelatin. Invasive protrusions of cells on Oregon Green® 488-conjugated-gelatin were analyzed as described in a previous report [21].

2.8. Statistical methods

Student's *t*-tests were performed for comparisons of mean values to determine significance. p values <0.05 were considered significant.

3. Results

3.1. The C-terminal tail of TM4SF5 bound and regulated c-Src family kinases (SFKs)

To study TM4SF5-mediated intracellular signaling, the intracellular regions of TM4SF5 were analyzed for binding to cell adhesion-related molecules using a peptide pull-down approach. Peptides of the cytosolic N- and C-terminal domains, or the intracellular loop (ICL) were separately mixed with whole cell extracts of SNU449 hepatoma cells. Interestingly, FAK and talin bound the ICL of TM4SF5 (Fig. 1A, and [20]), but SFK (*i.e.*, Src family kinases because the c-Src antibody recognized the members of c-Src, fyn, and yes) bound the C-terminal tail (Fig. 1A). Additionally, ectopic Myc-$(His)_6$-TM4SF5 co-immunoprecipitated with c-Src, whereas control normal IgG did not (Fig. 1B). The binding between TM4SF5 and SFKs in suspended cells was slightly stronger than that in adherent cells (Fig. 1C). SFKs still bound to the ICL deletion mutants of TM4SF5 (ΔICL13 or ΔICL19 whose 13 or 19 amino acids of 23 amino acid ICL were deleted, respectively), whereas FAK did not bind TM4SF5ΔICL19 (Fig. 1D). As expected, based on the observation that the C-terminal tail of TM4SF5 does not include tyrosine residues or proline-enriched domains, *in vitro* pull down using GST-c-Src WT or fragments and TM4SF5 peptides showed that GST-c-Src WT bound only the C-terminal peptide, but other GST-c-Src SH_2, SH_3, or SH_2SH_3 fragments did not (Fig. 1E). These data indicate that c-Src interacts with the C-terminal tail of TM4SF5 *via* regions other than its SH_2SH_3 domain.

Because suspended cells showed an interaction between TM4SF5 and SFKs, we examined whether the phosphorylation status of c-Src might affect its binding with TM4SF5. TM4SF5-null SNU761 cells were transiently cotransfected with Myc-$(His)_6$-TM4SF5 and either the $(HA)_3$-c-Src WT, Y416F, or Y527F mutant, before immunoprecipitation with $(His)_6$ antibody followed by Western blotting for the $(HA)_3$ tag. Interestingly, inactive Y416F c-Src more effectively bound to TM4SF5, compared with WT or active Y527F c-Src (Fig. 1F). Additionally, kinase-dead K295R c-Src bound TM4SF5 comparably to inactive Y416F c-Src (Fig. 1G).

To reveal the biological significance of the interaction, we generated C-terminus-deleted TM4SF5 ($TM4SF5_{\Delta C}$) and checked signaling activities after stable transfection of mock, WT, or $TM4SF5_{\Delta C}$. Although WT TM4SF5 expression increased Tyr416 c-Src phosphorylation (*i.e.*, pY^{416}c-Src), pY^{397}FAK, pY^{577}FAK, and pY^{486}cortactin, $TM4SF5_{\Delta C}$ expression further increased their phosphorylations, compared with mock or WT expression (Fig. 2A). Additionally, both TM4SF5 WT and $TM4SF5_{\Delta C}$ decreased the inhibitory phosphorylation on Tyr527 of c-Src (*i.e.*, pY^{527}c-Src, Fig. 2A). Furthermore, $TM4SF5_{\Delta C}$ transfection greatly enhanced pY^{486}cortactin regardless of whether inactive Y416F or active Y527F c-Src constructs were cotransfected presumably because of over-activated endogenous c-Src. However, Y527F c-Src cotransfection was required for a significant cortactin phosphorylation when TM4SF5 WT was transfected (Fig. 2B). When localizations of TM4SF5 and Tyr527-phosphorylated (*i.e.*, inactive) c-Src were determined by immunostaining, pY^{527}c-Src in WT TM4SF5 cells was positive at certain areas of lamellipodia but not completely along the leading edges ($63 \pm 4.7\%$), and pY^{527}c-Src in $TM4SF5_{\Delta C}$ cells was hardly observed along the leading edges ($87 \pm 6.2\%$, Fig. 2C). These observations may indicate that the interaction between TM4SF5 and either inactive or active c-Src leads to regulation of c-Src activity, presumably by limiting the location of inactive c-Src at certain leading edge areas during cell migration and invasion.

3.2. Tailless $TM4SF5_{\Delta C}$ enhanced migration and invasion

We next examined whether mock, TM4SF5 WT, and $TM4SF5_{\Delta C}$ cells differentially migrate or invade by using the transwell assay. TM4SF5 WT- and $TM4SF5_{\Delta C}$-transfected SNU449 hepatoma cells were efficiently migrated toward 10% fetal bovine serum (FBS) in the bottom chamber in a time-dependent manner compared with mock cells, although $TM4SF5_{\Delta C}$ cells migrated to a greater degree than TM4SF5 WT cells (Fig. 2D). However, the cells did not show significant migration toward bovine serum albumin (Fig. 2D, graph). Similarly, stable TM4SF5 WT and $TM4SF5_{\Delta C}$ SNU761 hepatoma cell lines also invaded efficiently through Matrigel toward 10% FBS in the bottom chamber, compared with control mock cells (Fig. 2E).

We next examined whether the enhanced migration of TM4SF5 WT and $TM4SF5_{\Delta C}$ hepatoma cells depended on c-Src. Using SYF fibroblasts (lacking c-Src, Fyn, and Yes) and SYF cells reconstituted with c-Src (SYF++, Fig. 2F) that express endogenous TM4SF5, we analyzed migration after transient transfection of mock, TM4SF5 WT, or $TM4SF5_{\Delta C}$. TM4SF5 WT- and $TM4SF5_{\Delta C}$-transfected SYF cells minimally migrated without any time-dependent increases, whereas TM4SF5 WT- and $TM4SF5_{\Delta C}$-transfected SYF++ cells dramatically increased migration toward 10% FBS compared with mock cells (Fig. 2G). Interestingly, $TM4SF5_{\Delta C}$-transfected SYF++ cells migrated more than did TM4SF5 WT-transfected SYF++ cells (Fig. 2G), being consistent with $TM4SF5_{\Delta C}$-transfected SYF++ cells showing higher pY^{416}c-Src than TM4SF5 WT-transfected SYF++ cells (Fig. 2F). These observations indicate that the C-terminal tail of TM4SF5 can

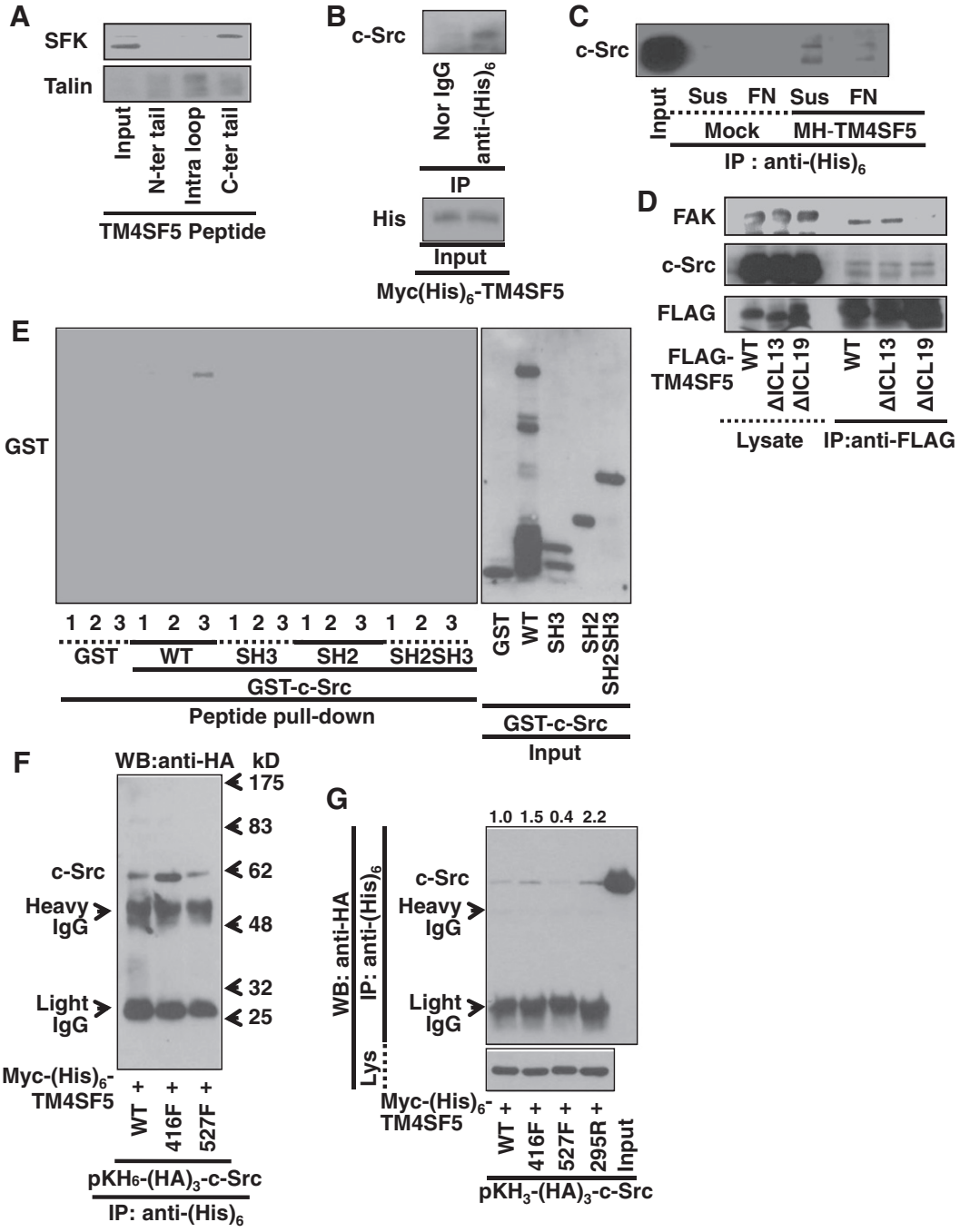

Fig. 1. The C-terminal tail of TM4SF5 bound SFK and regulated c-Src activity. (A) *In vitro* pull down using peptides of TM4SF5 cytosolic regions shows binding between the intracellular parts of TM4SF5, c-Src, and talin. N-ter, the NH_2-terminal tail of TM4SF5; Intra loop, the intracellular loop of TM4SF5; C-ter tail, C-terminal tail. (B) Extracts from myc-$(His)_6$-TM4SF5 (MH-TM4SF5)-transfected SNU449 cells were immunoprecipitated with either normal rabbit IgG (Nor. IgG) or anti-$(His)_6$ rabbit polyclonal antibody, prior to Western blots for c-Src or $(His)_6$-tag. (C) Cell extracts prepared from suspended (Sus) or replated on fibronectin (FN) for 2 h were immunoprecipitated with anti-$(His)_6$ antibody, prior to immunoblotting for c-Src. (D) SNU761 cells stably transfected with FLAG-TM4SF5 WT, ΔICL13, or ΔICL19 mutant were immunoprecipitated with FLAG antibody-precoated agarose beads, prior to immunoblottings for FAK, c-Src, or FLAG tag. (E) *In vitro* peptide pull down was performed by using peptides for the cytosolic regions of TM4SF5 and recombinant proteins of GST alone, GST-c-Src WT, SH_3 domain, SH_2 domain, and SH_2SH_3 domain, prior to immunoblotting for GST tag. (F and G) SNU761 cells were transiently cotransfected with Myc-$(His)_6$-TM4SF5 and either pKH_6-$(HA)_3$-c-Src WT, Y416F, Y527F (F), or K295R mutant (G) for 48 h, prior to harvests of whole cell extracts. The extracts were immunoprecipitated with anti-$(His)_6$ antibody and then immunoblotted for anti-$(HA)_3$ antibody. The band intensities among experimental conditions determined by image J are shown as relative values (G). Data represent three independent experiments.

bind c-Src and regulate its activity during TM4SF5-mediated cell migration and invasion.

3.3. TM4SF5 modulated invasive protrusions

To understand how TM4SF5 mediates invasion, we analyzed whether and how TM4SF5 might control invasive features such as invasive protrusions with activities to degrade the ECM. ECM degradation was visualized *via* microscopic observation of dark spots after the gelatin underneath cells was degraded by culturing cells on fluorophore-conjugated gelatin [2]. We first examined invasive protrusions between endogenously or exogenously TM4SF5-expressing and TM4SF5-null or -suppressed cells. SNU398, SNU449, and SNU761 hepatoma cell lines did not express TM4SF5, whereas SNU368, Huh7, and HepG2

hepatoma cell lines expressed TM4SF5 (Fig. 3A). When SNU398 and SNU368 cells were examined, TM4SF5-positive SNU368 cells formed invasive protrusions where fluorophore-conjugated gelatin was degraded to become dark spots, whereas TM4SF5-null SNU398 cells did not (Fig. 3B and E). Ectopic overexpression of TM4SF5 in SNU449 and SNU761 cells enhanced invasive protrusion formations, compared with mock transfected cells (Fig. 3C and E). Furthermore, suppression of endogenous TM4SF5 from Huh7 and HepG2 cells using sort hairpin RNA (shRNA) against TM4SF5 (shTM4SF5) did not form invasive protrusions, whereas a control shRNA against a scrambled sequence did (Fig. 3D and E). Compared with control mock cells, stable SNU761-TM4SF5 WT and SNU761-TM4SF5$_{\Delta C}$ cells showed a difference in formation of invasive protrusions; SNU761-TM4SF5$_{\Delta C}$ cells were more efficient than SNU761-TM4SF5 cells (Figs. 3F and S1). These data suggest that TM4SF5 expression indeed enhances invasion *via* effectively invasive protrusions.

3.4. TM4SF5-mediated invasive protrusions required c-Src WT in addition to (in)active c-Src

We next examined whether TM4SF5 WT- and TM4SF5$_{\Delta C}$-mediated invasive protrusion formation also depended on c-Src. Suppression of

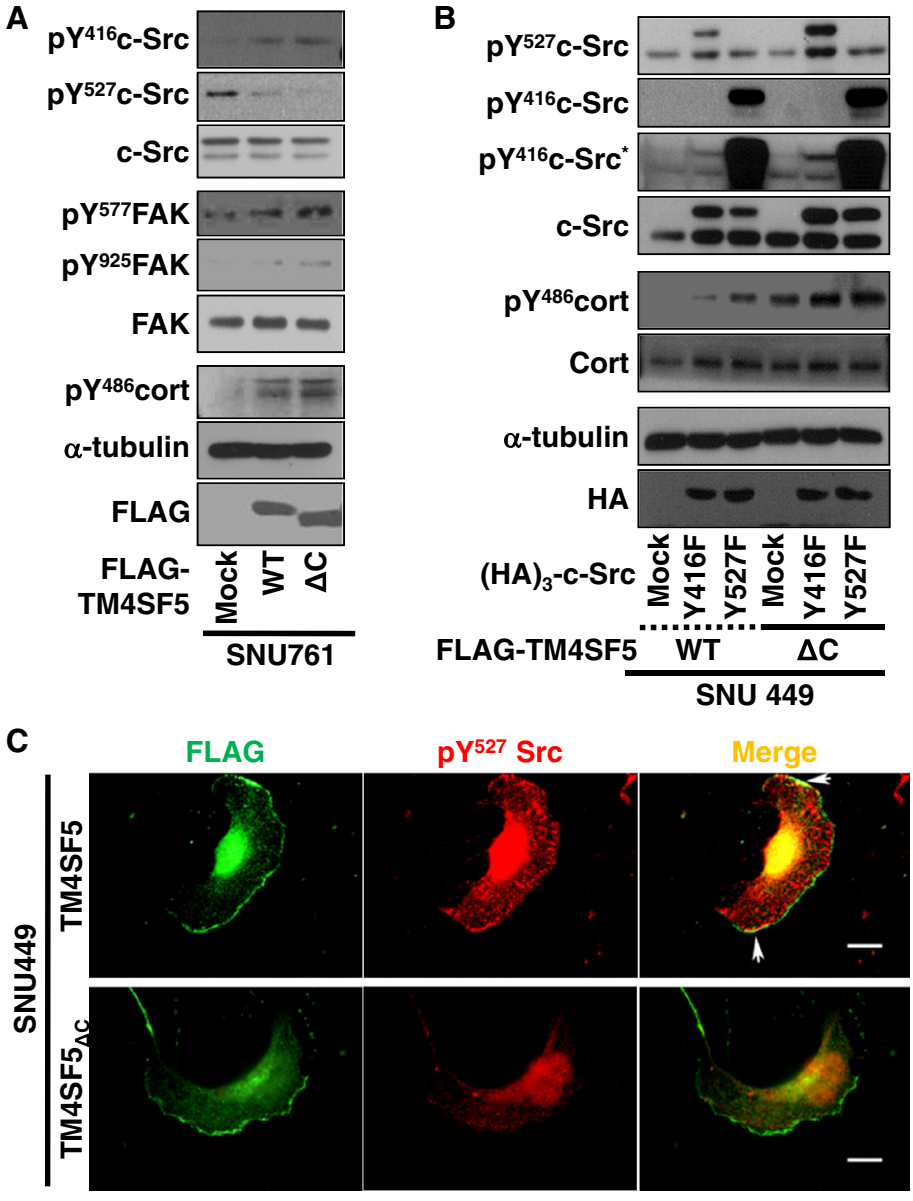

Fig. 2. C-terminal deletion mutant of TM4SF5 enhance migration and invasion. (A) Subconfluent SNU761 cells stably expressing mock, TM4SF5 WT, or TM4SF5$_{\Delta C}$ were harvested for immunoblots for the indicated molecules. (B) SNU449 cells were cotransfected with TM4SF5 WT or TM4SF5$_{\Delta C}$ (ΔC) and either mock, (HA)$_3$-c-Src Y416F or Y527F mutant for 48 h, before standard Western blots. (C) SNU449 cells were transfected with TM4SF5 WT or TM4SF5$_{\Delta C}$ for 48 h, prior to processing to indirect immunofluorescence microscopy using anti-FLAG (green) or -pY^{527}c-Src (red) antibodies. Scale for 10 μm. (D and E) SNU449 (D) or SNU761 (E) cells were transiently or stably, respectively, transfected with either mock, TM4SF5 WT, or TM4SF5$_{\Delta C}$ constructs. The cells were used in assay of transwell migration toward 10% FBS or BSA (as a control) in the bottom chamber for 12 or 16 h (D) or of transwell invasion through matrigel with 10% FBS in the bottom chamber for 24 h (E). At least 5 random images for migrated or invaded cells were recorded for each condition and numbers of migrated or invaded cells were counted for mean ± standard deviation values (graphs). (F and G) SYF or SYF++ cells were transiently transfected with either mock, TM4SF5 WT, or TM4SF5$_{\Delta C}$ constructs for 48 h, prior to harvests and standard Western blots for the indicated molecules (F) or processed transwell migration assay toward 10% FBS in the bottom chamber for 12 or 24 h (G). The band intensities among experimental conditions determined by image J are shown as relative values (F). (Graph) At least 5 random images for migrated cells were recorded for each condition and cell numbers were counted for mean ± standard deviation values. p values < 0.05 (*) or < 0.001 (**) are considered significant, compared with its control counterpart. Data represent three independent experiments.

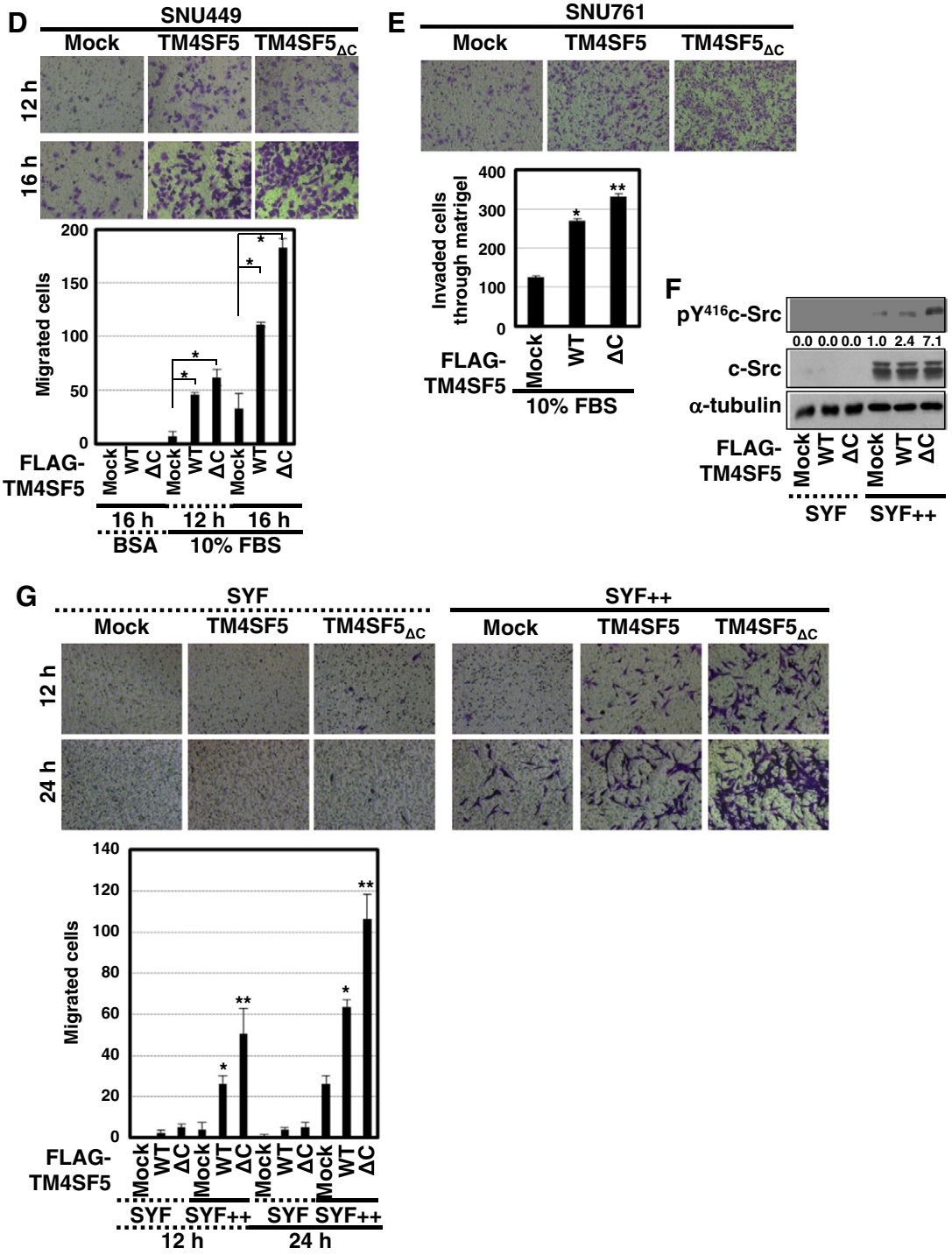

Fig. 2 (*continued*).

c-Src from stable SNU761 cells using its siRNA efficiently inhibited invasive protrusion formation (Fig. 4A and B). Such c-Src-dependent invasive protrusion formation in stable TM4SF5 WT or TM4SF5$_{\Delta C}$ cells were also confirmed using SYF or SYF++ fibroblasts. Although SYF cells transfected with either mock, TM4SF5 WT, or TM4SF5$_{\Delta C}$ did not form invasive protrusions, SYF++ cells transfected with TM4SF5 WT or TM4SF5$_{\Delta C}$, but not with mock, efficiently formed invasive protrusions: TM4SF5$_{\Delta C}$-transfected SYF++ cells were more efficient to form the protrusions than TM4SF5 WT-transfected cells (Figs. 4C and S2). These results suggest that TM4SF5 WT and TM4SF5$_{\Delta C}$ cells require c-Src to form invasive protrusions.

Because we found that TM4SF5 mediated formation of invasive protrusions (Fig. 3) and TM4SF5 bound inactive c-Src, we speculated that the phosphorylation status of c-Src either at Tyr416 or Tyr527 affected invasive protrusion formation. To test this finding, SYF or SYF++ cells were transiently transfected with either Y416F or Y527F c-Src or cotransfected with both Y416F and Y527F c-Src (at a mole ratio of 1:1) before analysis of invasive protrusion formation. Interestingly, SYF cells transfected with any of the c-Src constructs did not efficiently form invasive protrusions (Figs. 4D and S3). However, SYF++ cells transfected with the constructs could significantly form the invasive protrusions. Cotransfection of both Y416F and

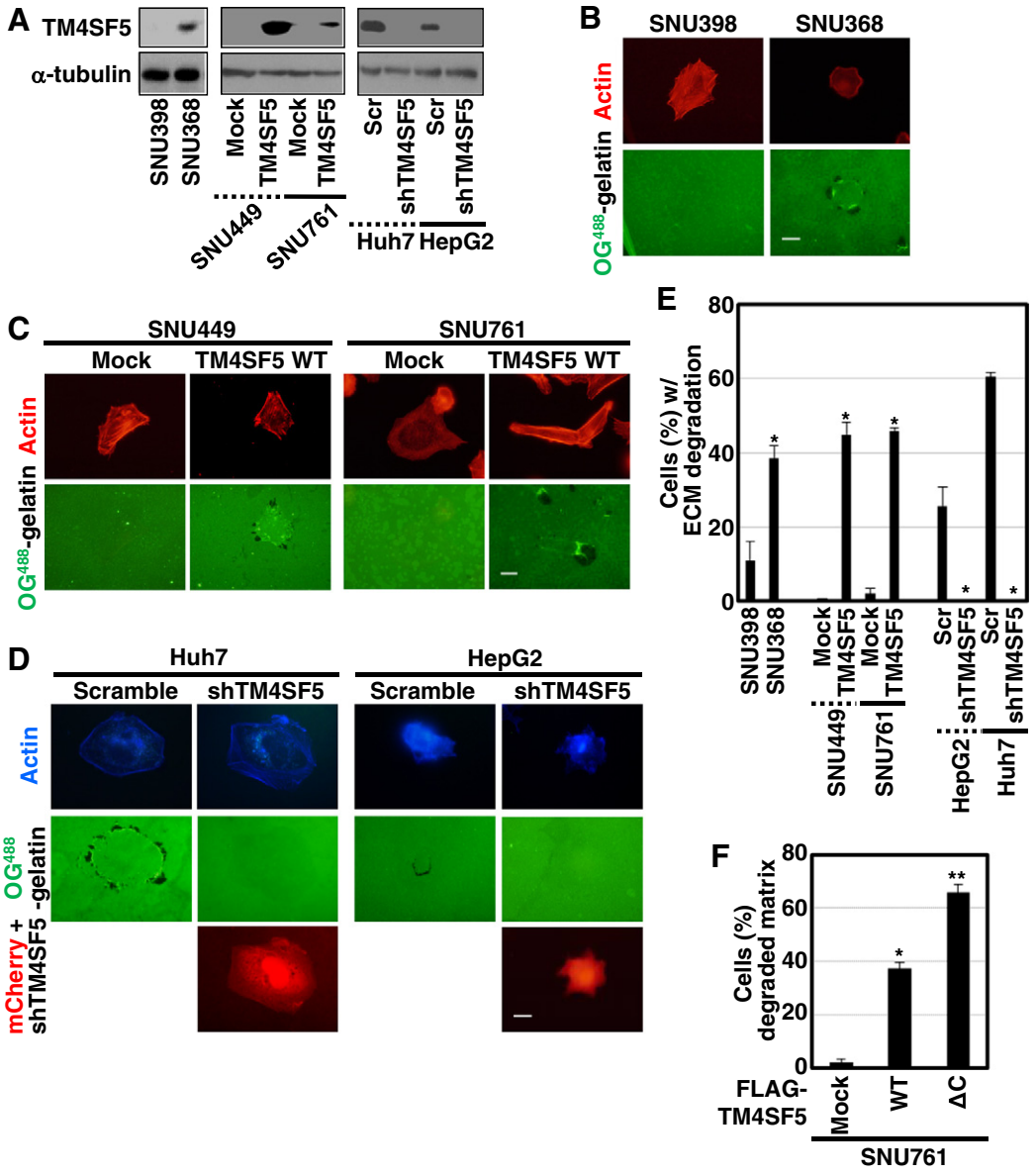

Fig. 3. TM4SF5 modulated invasive protrusions. (A to E) SNU398, SNU368 (B and E), SNU449 (stably transfected with mock or TM4SF5), SNU761 (stably transfected with mock or TM4SF5) (C and E), Huh7, or HepG2 (stably transfected with shRNA against a scrambled (Scr) sequence or TM4SF5 [shTM4SF5 [15]] cells (D and E) were harvested for immunoblots for TM4SF5 and α-tubulin (A), or analyzed for formation of invasive protrusions *via* culturing cells on Oregon Green® 488-conjugated gelatin for 30 h (B to D). Representative images without or with ECM-degraded spots (dark spots) were randomly saved for counting of cells in each experimental condition to quantitatively determine the levels of invasive protrusion formation (F). Cells more than at least 100 cells in each condition were saved and counted for mean ± standard deviation values. p values <0.05 (*) or <0.001 (**) are considered significant, compared with its control counterpart. Data represent three independent experiments.

Y527F c-Src showed greater formation of invasive protrusions than single transfection of either inactive Y416F or active Y527F c-Src (Fig. 4D). Interestingly, expression of inactive Y416F c-Src in SYF++ cells resulted in a slightly greater formation of invasive protrusions compared with active Y527F expression in SYF++ cells (Fig. 4D), although it is unclear how and why it occurred, or if the difference might not be biologically meaningful. These results strongly suggest that WT c-Src is required for TM4SF5-mediated formation of invasive protrusions, in addition to Tyr-(un)phosphorylated c-Src. When the c-Src constructs were transiently transfected into SNU761-mock or SNU761-TM4SF5 cells (with endogenous c-Src), single transfection of Y416F or Y527F c-Src and cotransfection of Y416F and Y527F c-Src caused efficient formation of invasive protrusions, being more dramatically enhanced in SNU761-TM4SF5 cells than in SNU761-mock cells (Figs. 4E and S4). Active Y527F c-Src transfection formed the protrusions approximately 50% more than did Y416F c-Src transfection, whereas cotransfection of Y416F and Y527F c-Src resulted in an intermediate level of invasive protrusion formation (Fig. 4E), although why the pattern between the c-Src constructs is different from that of SYF/SYF++ cell systems cannot currently be explained.

3.5. TM4SF5 WT formed invasive protrusions depending on growth factors, whereas TM4SF5$_{\Delta C}$ did independently

When signaling activities were examined in stable SNU761 cells, we interestingly found that EGFR phosphorylation in TM4SF5 WT or TM4SF5$_{\Delta C}$ cells was slightly or much higher, respectively, than in control mock cells (Fig. 5A, left 3 lanes). Because TM4SF5-mediated formation of invasive protrusions may involve EGFR phosphorylation,

we next checked the effects of serum deprivation on c-Src and EGFR phosphorylation. Compared with mock cells, TM4SF5 WT or TM4SF5$_{\Delta C}$ cells showed higher pY^{416}c-Src and pY^{845}EGFR, pY^{992}EGFR, and pY^{1173}EGFR; TM4SF5 WT cells showed increases in pY^{416}c-Src, pY^{845}EGFR, and pY^{992}EGFR in a serum-dependent manner, whereas TM4SF5$_{\Delta C}$ cells increased pY^{416}c-Src and EGFR phosphorylation with a

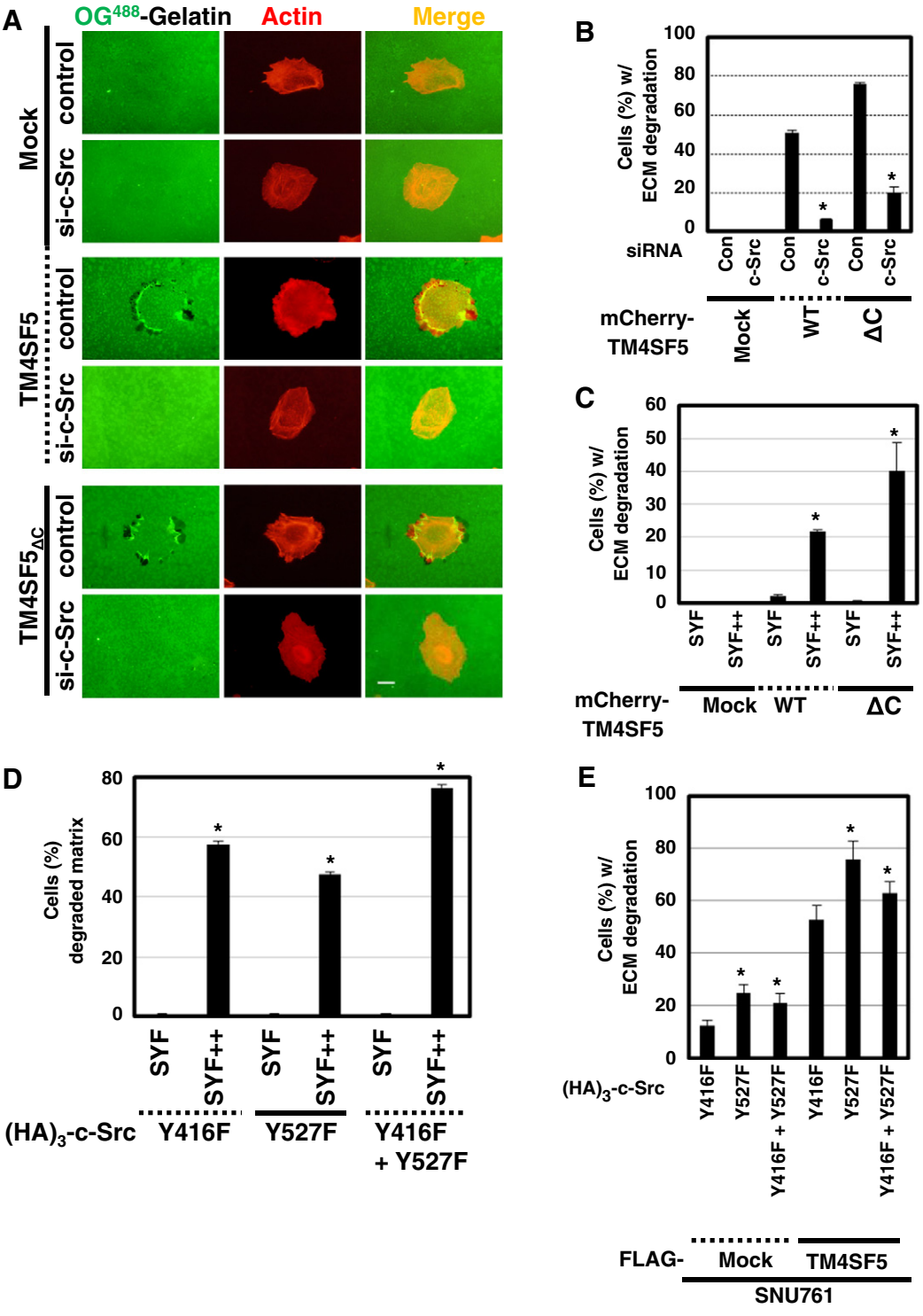

Fig. 4. TM4SF5-mediated invasive protrusions required c-Src WT in addition to (in)active c-Src. (A to E) Invasive protrusion formation was examined for stable SNU761 cells expressing mock, TM4SF5 WT, or TM4SF5$_{\Delta C}$ (A and B), for SYF, or SYF++ cells transiently transfected with mCherry-mock, mCherry-TM4SF5 WT, or mCherry-TM4SF5$_{\Delta C}$ constructs (C), or with (HA)$_3$-Y416F c-Src, (HA)$_3$-Y527F c-Src alone, or both (HA)$_3$-416 F c-Src and (HA)$_3$-Y527F c-Src for 24 h (D), for stable mock or SNU761-TM4SF5 cells transiently transfected with (HA)$_3$-Y416F c-Src, (HA)$_3$-Y527F c-Src alone, or both (HA)$_3$-416F c-Src and (HA)$_3$-Y527F c-Src for 24 h (E). The assay was performed culturing the cells on Oregon Green® 488-conjugated gelatin for 30 h before imaging the dark spots (to indicate degraded ECM) by fluorescence microscopy. Random images for more than 100 cells were saved for each experimental condition and cells with dark spots near or underneath cells were counted for mean ± standard deviation values. p values <0.05 (*) are considered significant, compared with its control counterpart. To show cell morphology and boundary, actin was also stained, as shown in the Supplemental figures. Data represent three independent experiments.

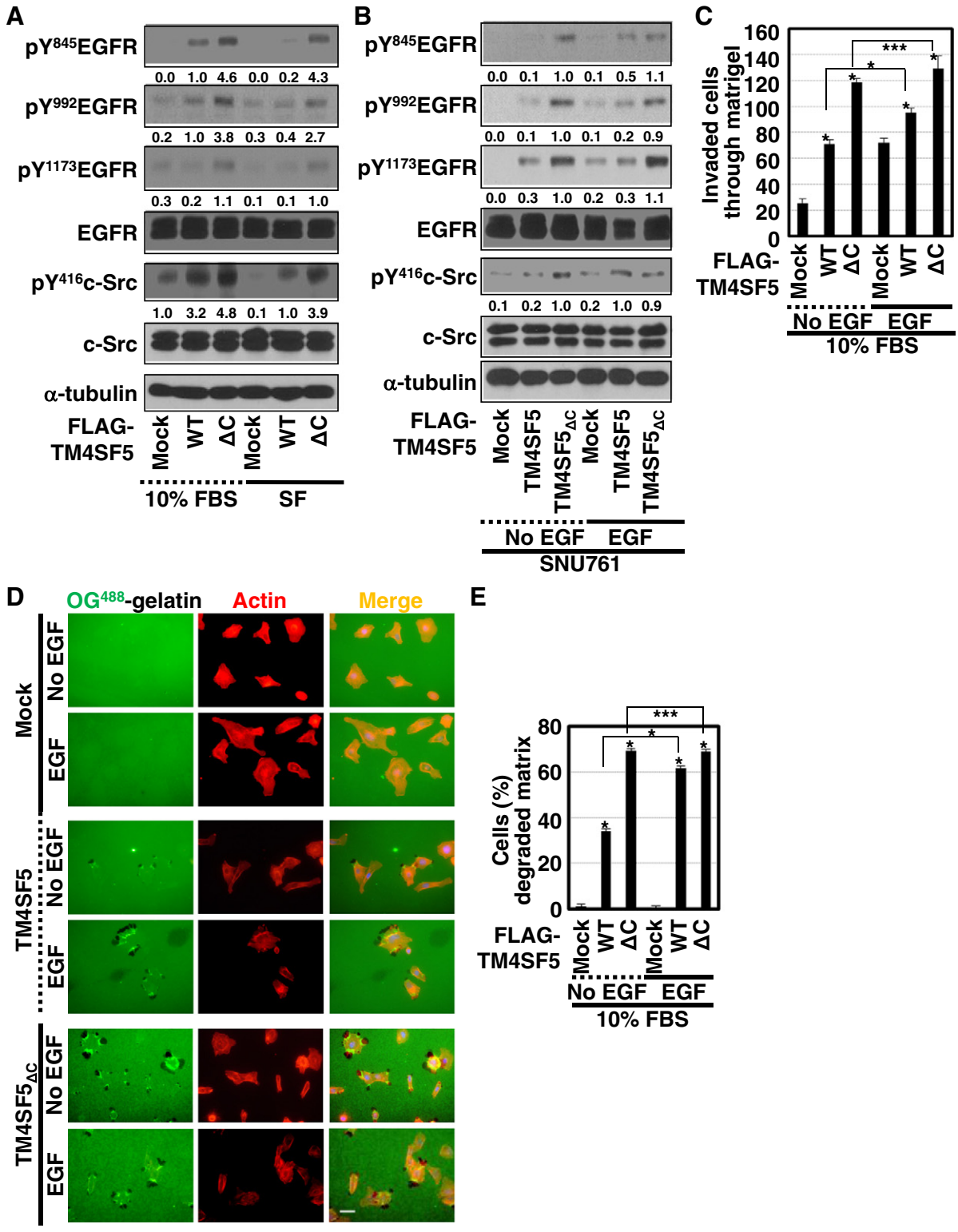

Fig. 5. TM4SF5 WT mediated invasive protrusion formation dependently on growth factors, whereas TM4SF5$_{\Delta C}$ did independently on growth factors. (A to B) Subconfluent SNU761 cells stably expressing mock, TM4SF5 WT, or TM4SF5$_{\Delta C}$ in normally 10% FBS containing culture condition (10% FBS) or serum-starved (SF) culture media overnight (A), treated without or with 100 ng/ml EGF in the presence of 10% FBS (B) for 24 h, were harvested for standard Western blots. The band intensities in each immunoblotting determined by image J are shown as relative values. (C to E) Stable SNU761 cells expressing mock, TM4SF5 WT, or TM4SF5$_{\Delta C}$ were analyzed for transwell migration (C) or for formation of invasive protrusions (D and E) toward 10% FBS ± EGF for 24 h or 30 h, respectively. Random images for more than 100 cells were saved and cells migrated were counted for mean ± standard deviation values (C and E). *p* values<0.05 (*) or ≥0.05 (***) are considered significant or insignificant, compared with its control counterpart, respectively. Data represent three independent experiments.

less serum dependency compared with mock cells (Fig. 5A). This case was also valid when the cells were treated with or without EGF: TM4SF5 WT cells showed increased pY^{416}c-Src, pY^{845}EGFR, and pY^{992}EGFR in an EGF-dependent manner, whereas TM4SF5$_{\Delta C}$ cells showed the increases independent of EGF (Fig. 5B). Because pY^{416}c-Src and pY^{845}EGFR in TM4SF5 WT cells depended on serum or EGF,

pY^{845}EGFR appeared more relevant to c-Src activity, which may be responsible for the invasive protrusion formation difference between TM4SF5 WT and TM4SF5$_{\Delta C}$ cells.

To distinguish the difference in dependency of TM4SF5 WT and TM4SF5$_{\Delta C}$ cells on serum or EGF treatment, we analyzed invasion through Matrigel and formation of invasive protrusions under an experimental condition including 10% FBS ± EGF. In the presence of 10% FBS alone, TM4SF5 WT and TM4SF5$_{\Delta C}$ cells showed enhanced invasion through the Matrigel, compared with mock cells (Figs. 5C and S5). Additional EGF treatment increased invasion of mock and TM4SF5 WT cells but not that of TM4SF5$_{\Delta C}$ cells (Figs. 5C and S5). That is, TM4SF5$_{\Delta C}$ cells showed an invasion capacity independent of additional EGF treatment. This was also valid for invasive protrusion formation. When mock cells did not show formation of invasive protrusions with or without EGF treatment, TM4SF5 WT and TM4SF5$_{\Delta C}$ cells showed efficient formation of invasive protrusions. TM4SF5 WT cells showed an EGF-dependent increase, whereas TM4SF5$_{\Delta C}$ cells formed invasive protrusions in an EGF-independent manner (Fig. 5D and E).

3.6. TM4SF5-mediated invasive protrusions required c-Src and Tyr845 phosphorylation of EGFR

Because TM4SF5 WT and TM4SF5$_{\Delta C}$ cells showed increased pY^{416}c-Src, pY^{845}EGFR, and invasive protrusion formation, we wondered how these effects were interconnected. We thus analyzed signaling activities of stable SNU761 cells transfected with control or c-Src siRNA. Suppression of c-Src abolished almost completely pY^{416}c-Src and pY^{845}EGFR, slightly pY^{992}EGFR, but not pY^{1173}EGFR in the cells (Fig. 6A). Thus TM4SF5-mediated invasive protrusion formation may likely involve c-Src-dependent EGFR Tyr845 phosphorylation. To test this finding, we transiently transfected Y845F EGFR into the stable SNU761 cells, prior to analysis of invasive protrusions.

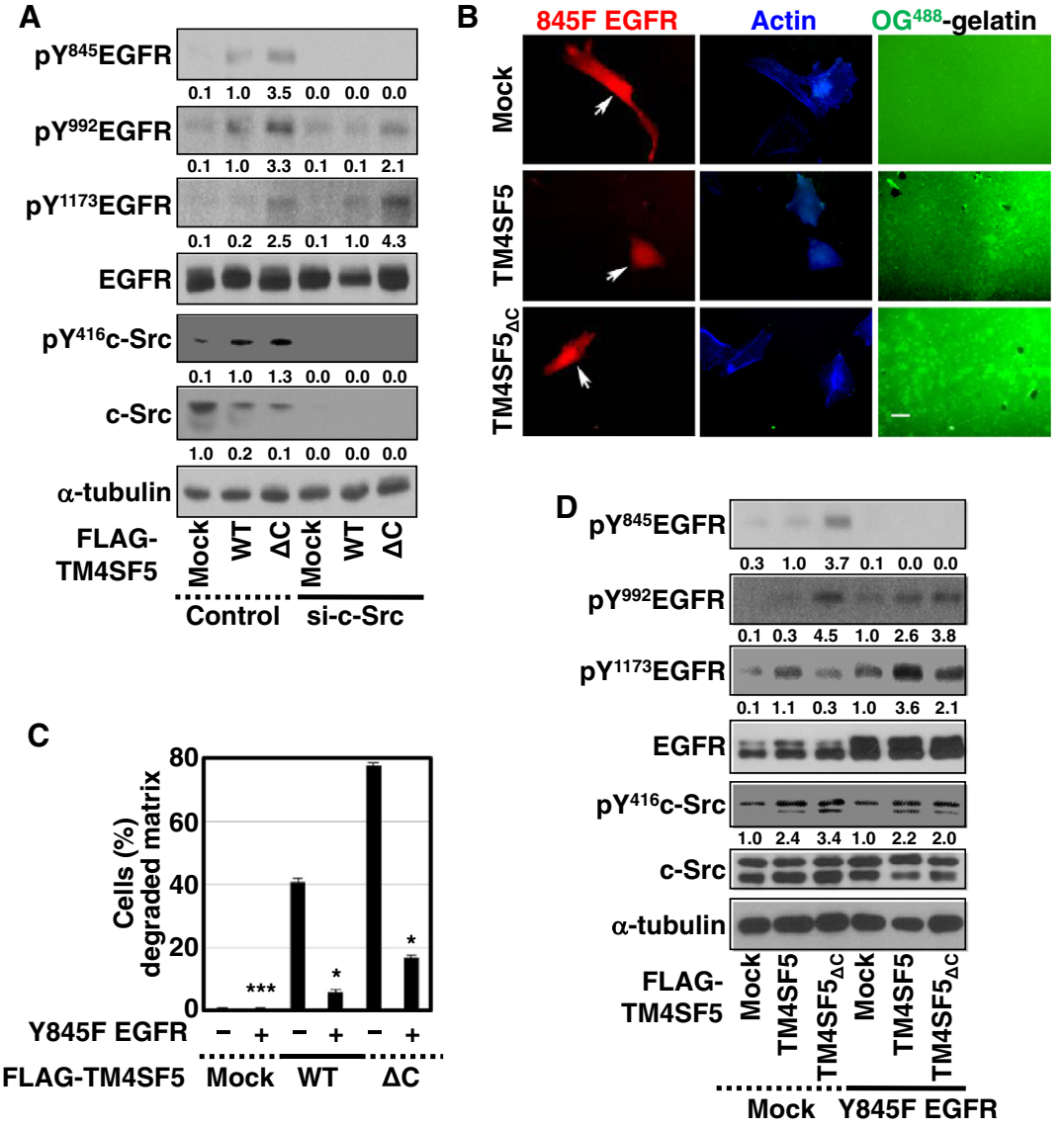

Fig. 6. TM4SF5-mediated invasive protrusions required c-Src and Tyr845 phosphorylation of EGFR. (A to D) Stable SNU761 cells expressing mock, TM4SF5 WT, or TM4SF5$_{\Delta C}$ were transiently transfected with siRNA against a control or c-Src (si-c-Src) for 48 h, prior to whole cell extract preparation for standard Western blots (A). Stable SNU761 cells were transiently transfected with mock or Y845F EGFR for 48 h, before analysis for invasive protrusion formation for 30 h (B and C) or before standard Western blots for the indicated molecules (D). Random images for more than 100 cells were saved and cells with dark spots were counted for mean ± standard deviation values (C). The band intensities in each immunoblotting determined by image J are shown as relative values (A and D). Data represent three different experiments.

Although mock cells did not form invasive protrusions in either Y845F EGFR-transfected or -untransfected cells, TM4SF5 WT and TM4SF5$_{\Delta C}$ cells formed significant invasive protrusions only when Y845F EGFR was not transfected (Fig. 6B, arrow and C). When Y845F EGFR was transfected, pY^{845}EGFR was abolished; however, pY^{992}EGFR and pY^{1173}EGFR were still enhanced in TM4SF5 WT and TM4SF5$_{\Delta C}$ cells, compared with mock cells (Fig. 6D). These data indicate that TM4SF5-mediated c-Src activity can regulate the formation

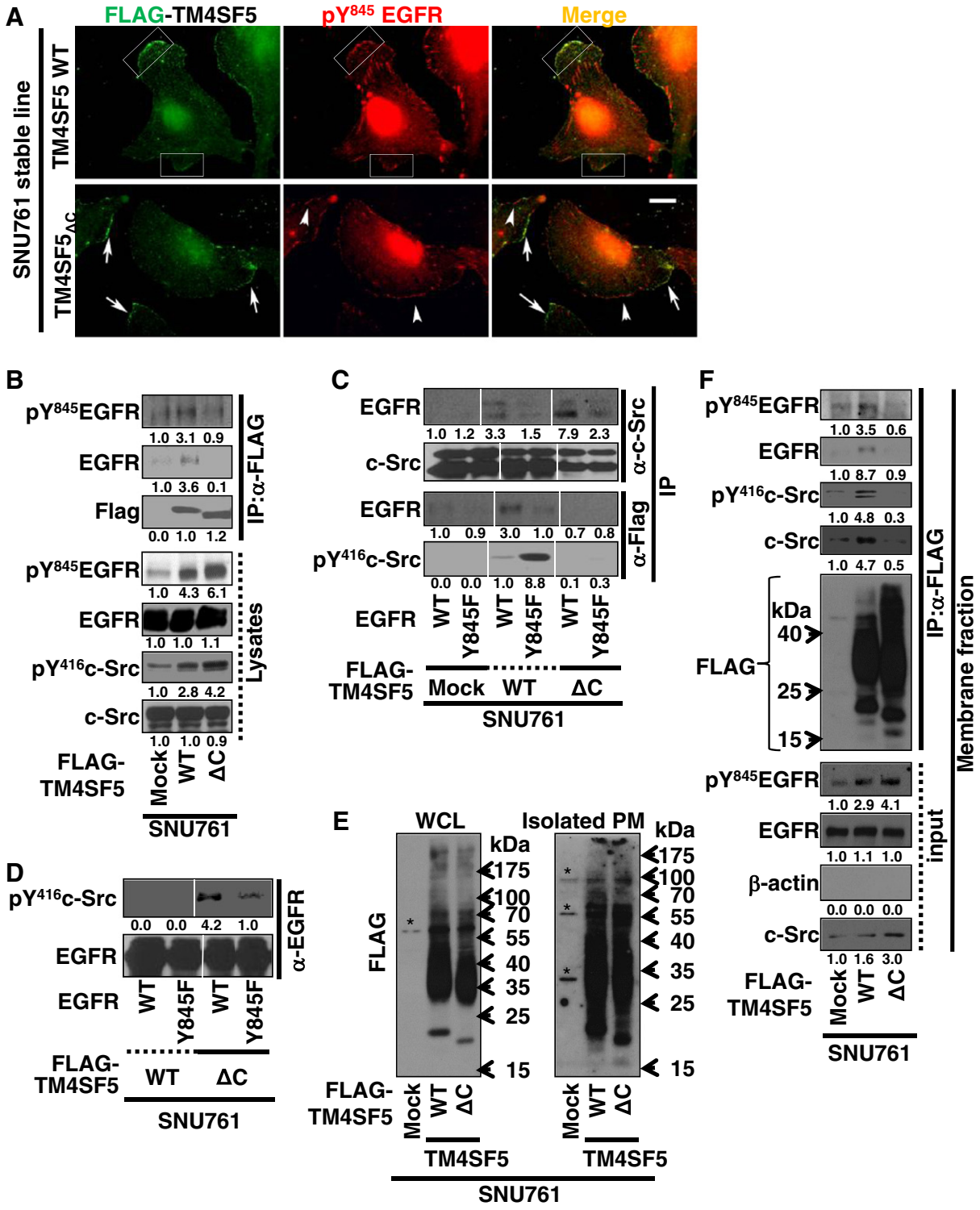

Fig. 7. TM4SF5-mediated invasive protrusions *via* TM4SF5/c-Src/EGFR pathway. (A and B) Stable SNU761 cells expressing FLAG-TM4SF5 WT, or FLAG-TM4SF5$_{\Delta C}$ were processed to indirect immunofluorescence (A) or prepared cell extracts for immunoprecipitation and standard Western blots. Lysates (Lys) were also blotted (B). (C and D) The extracts from the stable SNU761 cells transfected with EGFR WT or Y845F mutant for 48 h, were immunoprecipitated (IP) with FLAG antibody-precoated agarose beads (lower panel of C), anti-c-Src antibody (upper panel of C), or -EGFR antibody (D), before standard Western blots for c-Src, EGFR, or pY^{416}c-Src. (E and F) The plasma membrane (PM) factions (E) or membrane fractions (F) were isolated from SNU761 cells expressing either mock, FLAG-TM4SF5 WT, or FLAG-TM4SF5$_{\Delta C}$, by following the manufacturers' protocols, prior to immunoblottings against the indicated molecules (E) or immunoprecipitation with anti-FLAG antibodies for the standard Western blots using antibodies against the indicated molecules (F) in parallel with input (membrane fraction). The band intensities in each immunoblotting determined by image J are shown as relative values (B, C, D, and F). Data represent three isolated experiments.

of invasive protrusions *via* an increase in Tyr845 phosphorylation of EGFR.

3.7. TM4SF5-mediated invasive protrusions via the TM4SF5/c-Src/EGFR pathway

The relationship among TM4SF5, c-Src, and EGFR was further investigated. Stable SNU761-TM4SF5 or -TM4SF5$_{\Delta C}$ cells transfected with Y845F EGFR were analyzed for colocalization between TM4SF5 and pY^{845}EGFR. Interestingly, TM4SF5 WT-expressing cells showed colocalization of TM4SF5 and pY^{845}EGFR around lamellipodia, whereas they were separately localized in TM4SF5$_{\Delta C}$ cells (Fig. 7A). The interaction between TM4SF5 WT, but not TM4SF5$_{\Delta C}$, and pY^{845}EGFR was also confirmed by coimmunoprecipitation (Fig. 7B). When either EGFR WT or the Y845F mutant was transiently transfected into stable SNU761 cells, SNU761-mock cells did not show a detectable interaction between c-Src and EGFR, whereas SNU761-TM4SF5 or -TM4SF5$_{\Delta C}$ cells showed an obvious interaction between c-Src and EGFR WT, although SNU761-TM4SF5$_{\Delta C}$ cells showed a greater interaction. The interaction was obvious when EGFR WT was transfected, but it was much reduced when Y845F EGFR was transfected (Fig. 7C). Additionally, SNU761-TM4SF5 WT cells transfected with EGFR WT showed an interaction between FLAG-TM4SF5 and EGFR, but a minimal interaction between FLAG-TM4SF5 and pY^{416}c-Src, although SNU761-mock and TM4SF5$_{\Delta C}$ cells did not show interaction between FLAG-TM4SF5 and pY^{416}c-Src (Fig. 7C). Furthermore, Y845F EGFR transfection to FLAG-TM4SF5 WT cells reversed the coimmunoprecipitation pattern: interaction between FLAG-TM4SF5 and EGFR was markedly inhibited, whereas interaction between FLAG-TM4SF5 and pY^{416}c-Src was substantially increased after Y845F EGFR transfection (Fig. 7C). Thus, pY^{416}c-Src may likely more tightly bind to EGFR when Tyr845 can be phosphorylated, but to TM4SF5 when Tyr845 cannot be phosphorylated. Consistently, EGFR immunoprecipitates only from SNU761-TM4SF5$_{\Delta C}$ cells, but not from SNU761-TM4SF5 WT cells, pulled down pY^{416}c-Src when EGFR WT was transfected, whereas the interaction between EGFR and pY^{416}c-Src was reduced in Y845F EGFR-transfected SNU761-TM4SF5$_{\Delta C}$ cells (Fig. 7D), indicating that (enhanced) pY^{845}EGFR is important for recruit of pY^{416}c-Src in SNU761-TM4SF5$_{\Delta C}$ cells. The isolated plasma membrane fraction showed similar levels of TM4SF5 WT and TM4SF5$_{\Delta C}$, indicating that the C-terminal deletion might not impair its trafficking to the plasma membrane (Fig. 7E). Immunoprecipitation of FLAG-TM4SF5 in the membrane fractions from SNU761 cells expressing mock, FLAG-TM4SF5 WT, or -TM4SF5$_{\Delta C}$ mutant co-precipitated pY^{845}EGFR and pY^{416}c-Src in SNU761-TM4SF5 WT cells but not SNU761-TM4SF5$_{\Delta C}$ cells (Fig. 7F). These colocalization and coimmunoprecipitation data support that TM4SF5 WT interacts with either pY^{527}c-Src (to limit inactive c-Src to certain areas where TM4SF5 localizes; Fig. 8, left) or pY^{416}c-Src to link signaling to pY^{845}EGFR for TM4SF5-mediated cortactin activation and invasive protrusion formation (Fig. 8, middle). The C-terminal tail of TM4SF5 may likely regulate c-Src activity; thus, in TM4SF5$_{\Delta C}$ cells, c-Src is somehow (see Discussion) activated and recruited to pY^{845}EGFR for more efficient invasive protrusion formation (Figs. 8, right and up, and 6). However, when pY^{845}EGFR is not available, active c-Src bound mostly to TM4SF5 but not to EGFR; no signal linkage from TM4SF5 to EGFR might lead presumably to less effective invasion (Figs. 8, right and down, and 6).

4. Discussion

The present study demonstrates that the C-terminal tail of TM4SF5 binds and regulates c-Src, which is required for EGFR phosphorylation at Tyr845 and formation of invasive protrusions for an enhanced invasion. Because TM4SF5 is highly expressed in hepatocarcinoma and plays roles in aberrant cell proliferation and enhanced metastatic potential [14], understanding of TM4SF5-mediated intracellular signal pathways would be important for development of therapeutic reagents against tumorigenesis mediated by TM4SF5 or -related signaling molecule(s). The present study suggests that the C-terminus-mediated regulation of c-Src (family kinase) activity can be targeted to inhibit invasion of TM4SF5-positive tumors, such as hepatocellular carcinoma.

The C-terminal tail of TM4SF5 consists of 11 amino acids without a specific protein subdomain. In the current study, we found that the C-terminal tail of TM4SF5 interacted with SFK *via* regions other than the SH_2SH_3 domain in c-Src. The C-terminus of TM4SF5 bound more efficiently to inactive or kinase-dead c-Src than active or Y416-phosphorylated c-Src, although active c-Src could still bind TM4SF5. The interaction between TM4SF5 and SFKs was more efficient in suspended cells (where c-Src would be generally inactive) than in adherent cells. The preferred binding between the C-terminus of

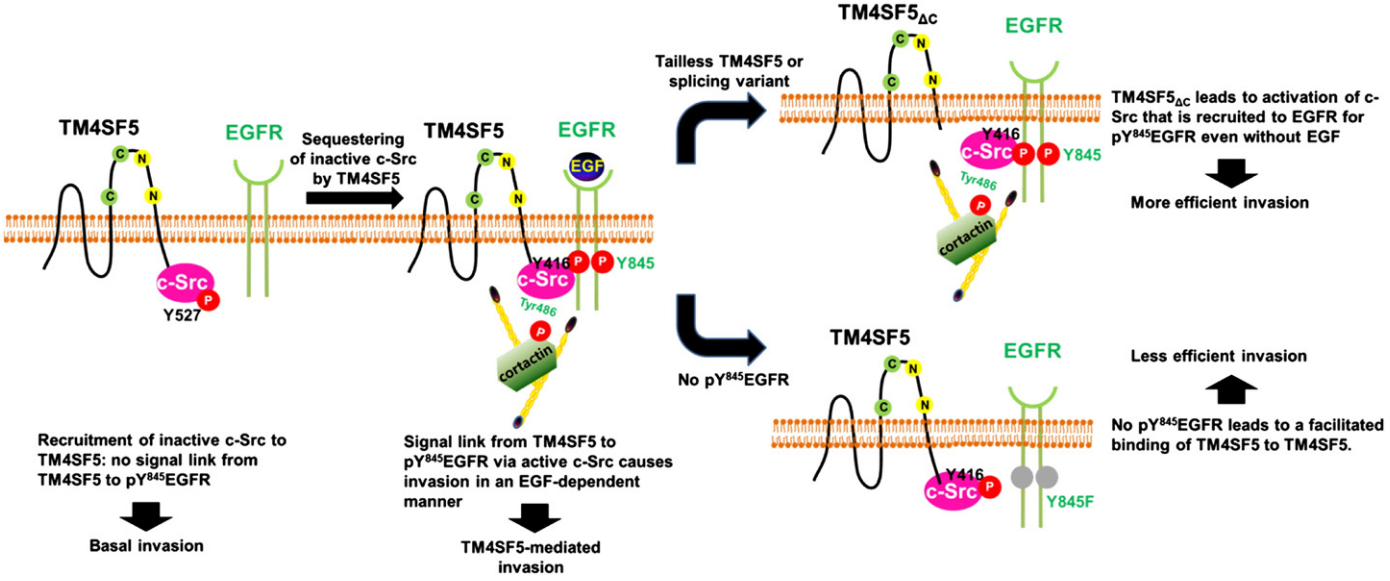

Fig. 8. Working model for TM4SF5-mediated regulation of c-Src activity and invasive protrusion formation.

TM4SF5 and inactive c-Src was unexpected, because we previously found that the ICL of TM4SF5 bound FAK to activate the actin-polymerizing machinery at the leading edges during a directional migration [20], and FAK/c-Src complex is well-known to control cell migration [22].

The interaction between the C-terminus of TM4SF5 and inactive SFKs may result in sequestration of inactive c-Src within certain locations during cell migration and invasion. The inactive (*i.e.*, pY^{527}c-Src) c-Src was located in certain peripheries of leading edges. At the locations of leading edges, inactive SFKs may limit activation of cortactin, a component of the actin-polymerizing machinery [10]. TM4SF5 could also bind active c-Src at leading edges with active formation of invasive protrusions. Active FAK is also recruited at the leading edges *via* binding to the ICL of TM4SF5 and forms a complex with molecules involved in the actin-polymerizing/branching machinery [20]. Therefore, even along the leading periphery of a migratory cell, there are possible regions with different capacities for actin polymerization and branching to direct dynamic cellular protrusions toward a specific direction.

TM4SF5 is a member of the tetraspan(in) family [13] that localizes to a specific membrane domain, the tetraspanin enriched microdomain (TERM or TEM) [11]. At the TERM, tetraspan(in)s form complexes with other tetraspan(in)s, integrins, or growth factor receptors [23]. Such massive complexes may transduce signals for diverse biochemical processes such as local actin polymerization and branching. *Via* physical interactions with other membrane receptors, tetraspan(in)-like TM4SF5 can regulate membrane activities to form local protrusions or retractions, presumably depending on differential microenvironments near the membrane [14]. Consistently, the membrane fraction from TM4SF5 WT-expressing cells showed complex formation among TM4SF5, (pY845)EGFR, and (pY416)c-Src, whereas the membrane fraction from tailless $TM4SF5_{\Delta C}$ cells did not show complex formation between tailless $TM4SF5_{\Delta C}$ and (pY845)EGFR (Fig. 7F). pY^{845}EGFR and invasive protrusion formation in TM4SF5 WT cells were further dependent on serum or EGF treatment. However, tailless $TM4SF5_{\Delta C}$ cells were independent of serum or EGF treatment and showed c-Src overactivation. We observed that active c-Src bound to a complex between TM4SF5 and EGFR WT (Fig. 7C and D). Active c-Src minimally bound to TM4SF5 WT when EGFR was phosphorylated at Tyr845, but much more bound to TM4SF5 WT when EGFR was not phosphorylated at Tyr845 (Fig. 7C). Thus, there must be at least two separate complex groups along the leading edges: one may consist of TM4SF5 and inactive SFKs to limit protrusion formation and the other may contain TM4SF5, active c-Src(/FAK), and pY^{845}EGFR to promote invasive protrusions.

The observations in the current study may support a role for the C-terminus of TM4SF5 in the regulation of SFKs. C-terminal deletion of TM4SF5 activated SFKs greater than TM4SF5 WT (Figs. 2, 5, 6 and 7B), suggesting its negative regulatory role in SFK signaling. The C-terminal peptide of TM4SF5 bound more efficiently to inactive c-Src than active c-Src (Fig. 1), although its underlying mechanisms remains unclear and its understanding may thus need details in structural aspects. We observed that more c-Src was found in the membrane fraction of $TM4SF5_{\Delta C}$ cells (*i.e.*, active c-Src on membrane [24], Fig. 7F), and inactive c-Src localized on certain membrane areas (Fig. 2C). Therefore, removal of the C-terminus of TM4SF5 might result in a less recruitment of inactive c-Src to the leading edges. It may be speculated that a certain population of TM4SF5 may sequester inactive c-Src around certain membrane areas rather than leading edges, although investigation in detail on such a possibility remains. c-Src activity in TM4SF5 or $TM4SF5_{\Delta C}$ cells correlated with pY^{845}EGFR (Figs. 6 and 7), and c-Src suppression abolished pY^{845}EGFR (Fig. 6A). Furthermore, a stronger association between active c-Src and pY^{845}EGFR in $TM4SF5_{\Delta C}$ cells than in TM4SF5 WT cells was observed (Fig. 7C and D). pY^{845}EGFR is a c-Src phosphorylation site even without ligand binding [25]. Y845F EGFR transfection did not alter c-Src activity but inhibited formation of invasive protrusions of TM4SF5 WT and $TM4SF5_{\Delta C}$ cells, suggesting a signaling link from c-Src to EGFR for invasive protrusion formation. $TM4SF5_{\Delta C}$ cells may thus acquire c-Src activation even without growth factor stimulation and result in more signal linkage for invasive protrusions.

SYF cells lacking SFKs or cells with c-Src suppression showed minimal pY^{845}EGFR and invasive protrusions. Invasive protrusions in TM4SF5 WT or $TM4SF5_{\Delta C}$ cells required expression of c-Src WT in addition to active and/or inactive c-Src. It was previously reported that active c-Src alone in head and neck squamous cell carcinoma results in invadopodia formation but not significant ECM degradation, whereas WT c-Src (which may convert to inactive and/or active c-Src form inside cells) caused efficient invadopodia maturation and ECM degradation [26]. Another previous study showed that v-Src overexpression into MtLN3 breast cancer cells results in less ECM degradation per invadopodia [27]. Active or inactive c-Src inside cells, which may be converted from WT c-Src depending on signaling contexts, may be differentially involved in complicate processes including invadopodia maturation (via an action of active c-Src) and ECM degradation (via invadopodia maturation by an action of WT c-Src) [26]. Therefore, c-Src WT form, but not active or inactive c-Src form only, led to efficient ECM degradation. The difference in c-Src requirement for the ECM degradation in hepatoma cell lines (the present study) and MtLN3 cells may be due to differential expression levels of molecule(s) involved in ECM-degradation *via* formation of invasive protrusions or invadopodia, such as TM4SF5.

In conclusion, the present study demonstrated that the C-terminal tail of TM4SF5 can regulate SFK activities *via* direct binding, which in turn can lead to Tyr845 phosphorylation of EGFR during formation of invasive protrusions along invasive peripheries and suggests that TM4SF5 may be targeted to inhibit the invasion of TM4SF5-positive tumors.

Conflict of interest statement

None declared.

Acknowledgements

The National Research Foundation (NRF) of the Korean Ministry of Education, Sciences and Technology (MEST) of Korea for Tumor Microenvironment Global Core Research Center (GCRC) grant (2012-0004891), senior researchers program (Leap research, 2012-0005606), and Global Frontier Project grant (NRF-2012M3A6A4054271) to JWL; the Korean Health Technology R&D Project of the Ministry for Health, Welfare and Family Affairs (MHWFA, A100727) to JWL.

Appendix A. Supplementary data

Supplementary Figs. 1 to 5 and Table 1 can be found at http://www.journals.elsevier.com/bba-molecular-cell-research/. Supplementary data associated with this article can be found, in the online version, at http://dx.doi.org/10.1016/j.bbamcr.2012.11.026.

References

[1] P. Friedl, K. Wolf, Proteolytic interstitial cell migration: a five-step process, Cancer Metastasis Rev. 28 (2009) 129–135.
[2] S. Linder, The matrix corroded: podosomes and invadopodia in extracellular matrix degradation, Trends Cell Biol. 17 (2007) 107–117.
[3] E.H. Danen, Integrin proteomes reveal a new guide for cell motility, Sci. Signal. 2 (2009) e58.
[4] M.D. Schaller, Cellular functions of FAK kinases: insight into molecular mechanisms and novel functions, J. Cell Sci. 123 (2010) 1007–1013.
[5] S.K. Mitra, D.D. Schlaepfer, Integrin-regulated FAK-Src signaling in normal and cancer cells, Curr. Opin. Cell Biol. 18 (2006) 516–523.
[6] P.A. Cole, K. Shen, Y. Qiao, D. Wang, Protein tyrosine kinases Src and Csk: a tail's tale, Curr. Opin. Chem. Biol. 7 (2003) 580–585.

[7] J. Foley, N.K. Nickerson, S. Nam, K.T. Allen, J.L. Gilmore, K.P. Nephew, D.J. Riese II, EGFR signaling in breast cancer: bad to the bone, Semin. Cell Dev. Biol. 21 (2010) 951–960.
[8] T.H. Leu, M.C. Maa, Functional implication of the interaction between EGF receptor and c-Src, Front. Biosci. 8 (2003) s28–s38.
[9] O. Destaing, M.R. Block, E. Planus, C. Albiges-Rizo, Invadosome regulation by adhesion signaling, Curr. Opin. Cell Biol. 23 (2011) 1–10.
[10] C. Albiges-Rizo, O. Destaing, B. Fourcade, E. Planus, M.R. Block, Actin machinery and mechanosensitivity in invadopodia, podosomes and focal adhesions, J. Cell Sci. 122 (2009) 3037–3049.
[11] M. Yanez-Mo, O. Barreiro, M. Gordon-Alonso, M. Sala-Valdes, F. Sanchez-Madrid, Tetraspanin-enriched microdomains: a functional unit in cell plasma membranes, Trends Cell Biol. 19 (2009) 434–446.
[12] F. Berditchevski, Complexes of tetraspanins with integrins: more than meets the eye, J. Cell Sci. 114 (2001) 4143–4151.
[13] M.D. Wright, J. Ni, G.B. Rudy, The L6 membrane proteins — a new four-transmembrane superfamily, Protein Sci. 9 (2000) 1594–1600.
[14] S.A. Lee, K.H. Park, J.W. Lee, Modulation of signaling between TM4SF5 and integrins in tumor microenvironment, Front. Biosci. 16 (2011) 1752–1758.
[15] S.A. Lee, S.Y. Lee, I.H. Cho, M.A. Oh, E.S. Kang, Y.B. Kim, W.D. Seo, S. Choi, J.O. Nam, M. Tamamori-Adachi, S. Kitajima, S.K. Ye, S. Kim, Y.J. Hwang, I.S. Kim, K.H. Park, J.W. Lee, Tetraspanin TM4SF5 mediates loss of contact inhibition through epithelial–mesenchymal transition in human hepatocarcinoma, J. Clin. Invest. 118 (2008) 1354–1366.
[16] Y.B. Kim, S. Choi, M.C. Choi, M.A. Oh, S.A. Lee, M. Cho, K. Mizuno, S.H. Kim, J.W. Lee, Cell adhesion-dependent cofilin serine 3 phosphorylation by the integrin-linked kinase.c-Src complex, J. Biol. Chem. 283 (2008) 10089–10096.
[17] H.-P. Kim, T.-Y. Kim, M.-S. Lee, H.-S. Jong, T.-Y. Kim, J. Weon Lee, Y.-J. Bang, TGF-β1-mediated activations of c-Src and Rac1 modulate levels of cyclins and p27Kip1 CDK inhibitor in hepatoma cells replated on fibronectin, BBA - Mol. Cell. Res. 1743 (2005) 151–161.
[18] S. Choi, S.A. Lee, T.K. Kwak, H.J. Kim, M.J. Lee, S.K. Ye, S.H. Kim, S. Kim, J.W. Lee, Co-operation between integrin α5 and tetraspan TM4SF5 regulates VEGF-mediated angiogenic activity, Blood 113 (2009) 1845–1855.
[19] M.A. Oh, S. Choi, M.J. Lee, M.C. Choi, S.A. Lee, W. Ko, W.G. Cance, E.S. Oh, L. Buday, S.H. Kim, J.W. Lee, Specific tyrosine phosphorylation of focal adhesion kinase mediated by Fer tyrosine kinase in suspended hepatocytes, BBA - Mol. Cell. Res. 1793 (2009) 781–791.
[20] O. Jung, S. Choi, S.-B. Jang, S.-A. Lee, S.-T. Lim, Y.-J. Choi, H.-J. Kim, D.-H. Kim, T.K. Kwak, H. Kim, M. Kang, M.-S. Lee, S.Y. Park, J. Ryu, D. Jeong, H.-K. Cheong, H.J. Kim, K.H. Park, B.-J. Lee, D.D. Schlaepfer, J.W. Lee, Tetraspan TM4SF5-dependent direct activation of FAK and metastatic potential of hepatocarcinoma cells, J. Cell Sci. (2012), http://dx.doi.org/10.1242/jcs.100586.
[21] S.A. Lee, T.Y. Kim, T.K. Kwak, H. Kim, S. Kim, H.J. Lee, S.H. Kim, K.H. Park, H.J. Kim, M. Cho, J.W. Lee, Transmembrane 4 L six family member 5 (TM4SF5) enhances migration and invasion of hepatocytes for effective metastasis, J. Cell. Biochem. 111 (2010) 59–66.
[22] V. Bolos, J.M. Gasent, S. Lopez-Tarruella, E. Grande, The dual kinase complex FAK-Src as a promising therapeutic target in cancer, Onco. Targets Ther 3 (2010) 83–97.
[23] M. Zoller, Tetraspanins: push and pull in suppressing and promoting metastasis, Nat. Rev. Cancer 9 (2009) 40–55.
[24] M.C. Frame, Src in cancer: deregulation and consequences for cell behaviour, Biochim. Biophys. Acta 1602 (2002) 114–130.
[25] D.A. Tice, J.S. Biscardi, A.L. Nickles, S.J. Parsons, Mechanism of biological synergy between cellular Src and epidermal growth factor receptor, Proc. Natl. Acad. Sci. U. S. A. 96 (1999) 1415–1420.
[26] L.C. Kelley, A.G. Ammer, K.E. Hayes, K.H. Martin, K. Machida, L. Jia, B.J. Mayer, S.A. Weed, Oncogenic Src requires a wild-type counterpart to regulate invadopodia maturation, J. Cell Sci. 123 (2010) 3923–3932.
[27] M. Oser, H. Yamaguchi, C.C. Mader, J.J. Bravo-Cordero, M. Arias, X. Chen, V. Desmarais, J. van Rheenen, A.J. Koleske, J. Condeelis, Cortactin regulates cofilin and N-WASp activities to control the stages of invadopodium assembly and maturation, J. Cell Biol. 186 (2009) 571–587.